Rare Met. (2014) 33(3):313–317
DOI 10.1007/s12598-014-0257-8

RARE METALS
www.editorialmanager.com/rmet

Mechanical properties of WC–Co coatings with different decarburization levels

Xu Wu*, Zhi-Meng Guo, Hai-Bin Wang, Xiao-Yan Song

Received: 11 February 2014 / Revised: 2 March 2014 / Accepted: 13 March 2014 / Published online: 25 April 2014

Abstract In this study, two kinds of WC–Co coatings with different decarburization levels were deposited by high-velocity oxy-fuel (HVOF) spraying using the ultrafine WC–Co composite powder and commercial micronsized powder, respectively. The hardness and elastic modulus were measured on the top surface and cross sections of the prepared coatings by the nanoindentation method. The results show that the ultrafine-structured coating has much higher density and inhibited decarburization than the conventional coating, which thus results in higher hardness and elastic modulus values than the micronsized coating. The wear resistance of thermal-sprayed cermet coatings greatly depends on the cross-sectional hardness and elastic modulus which reflects the bond strength between splats to some extent. Based on the analysis, a better understanding of the microstructure and properties in cermet coating materials was obtained.

Keywords Composite powder; Cermet coating; Decarburization; Nanoindentation; Wear resistance

1 Introduction

Thermal-sprayed WC–Co cermet coatings are widely used in the areas of aerospace, machinery, metallurgy, petroleum, and chemical industries because of their excellent mechanical properties such as high hardness, high wear resistance, and high erosion resistance [1–5]. For some particular applications, e.g., where the corrugating rolls are used to produce the corrugated board, higher hardness and better wear resistance are required for the working surface due to the continuous compression and abrasion of the paperboard and other hard particles during the production. Recent studies show that the wear resistance of the cermet coatings depends on their hardness and toughness to a great extent [6, 7]. The significant enhancement in the wear resistance of the cermet coating can be realized by improving its hardness and toughness. However, the decarburization of the carbides especially the ultrafine and nano-WC can hardly be avoided although the coating is deposited by the widely used high-velocity oxygen-fuel (HVOF) thermal-spraying technique, which thus results in the formation of brittle phases such as W_2C, W, and $Co_xW_yC_z$ and deteriorates the properties of the coating [8–10]. Babu et al. [11] found that as the decarburization level of the detonation-sprayed WC–Co coating increased from 4.5 % to 34 %, its surface hardness increased by 21 %, and the indentation fracture toughness was doubled. However, the abrasive wear resistance of the coating was hardly improved in the case of three abrasives with varying hardness values. As the decarburization level was further increased to 45 %, the coating hardness and toughness changed little, whereas the wear rate could be doubled while using either Al_2O_3 or SiC as the abrasive. Besides, their results did not show a definite relationship between the elastic modulus and the decarburization level of the coating. However, it can be found in Saha's results that the hardness and toughness measured on the coating cross section are strongly related with the decarburization level of the coating, as well as its wear resistance [12]. The reasons for this contradiction may come from the special splat structure in thermal-sprayed coatings,

X. Wu*, Z.-M. Guo
School of Materials Science and Engineering, University of Science and Technology Bejing, Beijing 100083, China
e-mail: wuxu.bjjs@163.com

H.-B. Wang, X.-Y. Song
College of Materials Science and Engineering, Beijing University of Technology, Beijing 100124, China

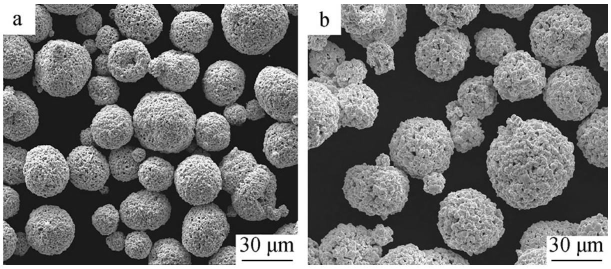

Fig. 1 SEM images of two kinds of WC–12Co feedstock powders: **a** ultrafine-structured feedstock powder provided by BJUT, and **b** commercial micronsized feedstock powder

which will result in obvious anisotropy on the top surface and cross section of coating. Until now, few researches have done to discuss how the mechanical parameters measured on coating surface and cross section affect the wear resistance of the coating. With respect to investigating this, two WC–Co coatings with different amounts of decarburization phases were deposited by HVOF-spraying system in the present work. Based on the analysis of the hardness and elastic modulus measured on the top surface and cross section of the prepared coatings by the nanoindentation method, the relationship between the decarburization level and the mechanical properties of the cermet coating was clarified.

2 Experimental

2.1 Feedstock powder

Two kinds of agglomerated and sintered WC–12Co feedstock powders were used. First, namely TYPE-1, was prepared using the in situ-synthesized ultrafine WC–12Co composite powder as the raw material [13], which was provided by Beijing University of Technology (BJUT). The feedstock was in the size range of 10–40 μm, as shown by Fig. 1a. The other powder, namely TYPE-2, was from Wuxi Xinke Surface Engineering Materials Co., Ltd., China. The size distribution is about 15–45 μm, as shown in Fig. 1b.

2.2 Coating deposition

The JP-5000 HVOF-spraying system made by PRAXAIR company in USA was used to deposit the coatings, and the respective optimized spraying parameters are listed in Table 1.

2.3 Coating characterization

The phases in the synthesized composite powder and HVOF-sprayed coatings were analyzed by X-ray diffraction (XRD) using Cu Kα radiation. The morphologies and microstructures of the powder particles and the coatings were observed by scanning electron microscopy (SEM). Nanoindentation hardness and modulus measurements were conducted on the polished top and cross-sectional surfaces of the coatings using Agilent Nano Indenter G200. The abrasive wear resistance of the WC–Co coatings was evaluated using dry sand rubber wheel abrasion test according to the ASTM-G65 standard. The specimens were ultrasonically cleaned in the absolute alcohol and weighed before and after each test. The tests were performed under a contact normal force of 130 N, a sand (Al_2O_3, ~220 μm) flow rate of 300 $g \cdot min^{-1}$, and a wheel rotating speed of 200 $r \cdot min^{-1}$. The volume wear rate of the specimens was converted from the measured mass loss after 6,000 revolutions of the rubber wheel.

3 Results and discussion

3.1 Microstructural analysis

Figure 2a and b shows the cross-sectional microstructures of the two HVOF-sprayed coatings, respectively. It can be seen that the coating prepared by the ultrafine composite powder significantly improves the density and uniformity, particularly with a homogeneous distribution of the hard carbide phases, while the coating prepared by the micronsized powder possesses many large pores. For the latter, a possible reason is that hard carbides particles in the micronsized powder were not heated well in the thermal-spraying flame, which leads to the insufficient spreading of the feedstock powder particles during their impact on the substrate. Consequently, the hard carbide phases are easy to be removed from the coating due to the weak bonding.

3.2 XRD analysis

Figure 3 shows the XRD results of the two coatings. With regard to the basic principle of HVOF spraying, it is known that the actual oxygen-fuel (OF) rate during the spraying

Table 1 HVOF-spraying parameters for two kinds of WC–12Co feedstock powders

Feedstock powder	Oxygen flow rate/ ($m^3 \cdot h^{-1}$)	Kerosene flow rate/ ($L \cdot min^{-1}$)	Powder feed rate/ ($g \cdot min^{-1}$)	Oxygen pressure/ MPa	Kerosene pressure/ MPa
Type-1	52.4	22.71	70	1.44	1.17
Type-2	56.6	23.46	76	1.44	1.17

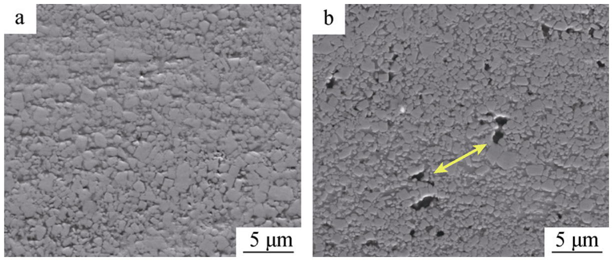

Fig. 2 SEM images of HVOF-sprayed WC–Co coating: **a** ultrafine-structured WC–Co coating and **b** conventional WC–Co coating

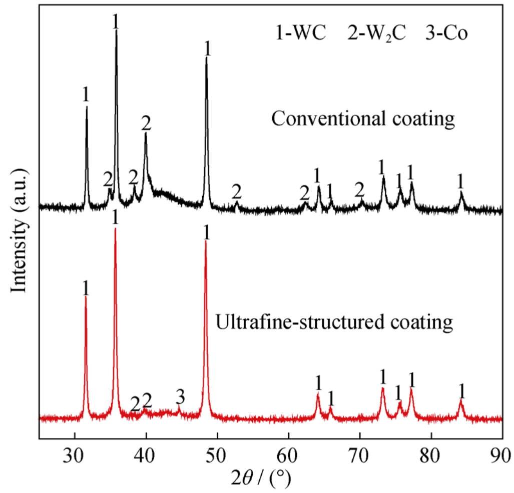

Fig. 3 XRD patterns of two HVOF-sprayed WC–Co coatings

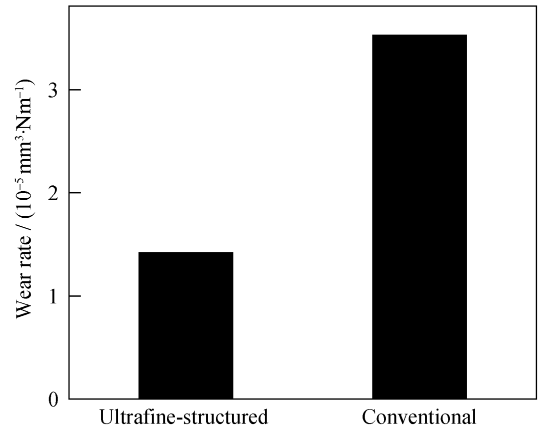

Fig. 4 Comparison of wear rates between two HVOF-sprayed WC–Co coatings

process is much higher than the stoichiometric ratio of complete combustion. Thus, the thermal-spraying flame always has excess oxygen, in which the WC decarburization can hardly be avoided. From Fig. 3, it can be seen that both the coatings have W_2C phases, whereas the micron-sized powder coating has many more. There are two possible reasons that account for this difference. For the feedstock powder prepared by the ultrafine WC–Co composite powder, the WC particles are almost clad with the Co matrix, and also a relatively higher density is obtained for the prepared feedstock (Fig. 1a), which reduces the tendency of exposure of WC particles to the ambient oxygen [14]. The other reason is the decreased oxygen-to-kerosene ratio for the spraying of the ultrafine composite powder. The reduction of oxidability of the flame results in the decrease of the content of W_2C phases in the coating.

3.3 Mechanical properties of the coatings

Under the same conditions, abrasive wear test was performed for the two coatings with different amounts of decarburized phases, as shown in Fig. 4. It is obvious that the ultrafine-structured WC–Co coating with lower decarburization exhibits better wear resistance. Particularly, the wear rate decreases by 60 % compared with the conventional coating. To find the reasons, the evaluations of hardness and elastic modulus were conducted on the polished coating surface and cross section by nanoindentation method [15]. The results are shown in Figs. 5 and 6, respectively. It can be found that the two coatings have almost the same surface hardness, whereas the average elastic modulus of the ultrafine-structured coating is 10 % higher than that of the conventional coating, which indicates that the ultrafine-structured coating has stronger elastic deformation resistance. During the wear test, the coating was subjected to the continuous extrusion stress and scratching of abrasives at a certain load. In local regions of the coating surface, the elastic deformation occurs at an earlier wear stage, and transforms into the plastic deformation with the applied load increasing, and the coating materials are finally removed after inner cracks formed. Therefore, the higher elastic modulus of the ultrafine-structured coating contributes to its higher wear resistance.

From the cross-sectional evaluation results, it can be seen that both the hardness and elastic modulus of the ultrafine-structured coating are obviously higher than those of the conventional coating. Also, it can be found from Fig. 6 that, the cross-sectional hardness and particularly the elastic modulus of both coatings decrease gradually with the indentation depth increasing, which is quite different from the surface indentation test curve. This can be explained by the stacking structure of the thermal-sprayed coatings. To some extent, the cross-sectional hardness and elastic modulus values of the coating determine the bond strength between splats. With the indentation depth increasing, cracks initiate in the local areas by decarburized phases, such as W_2C, which consequently results in the decrease of the cross-sectional elastic modulus. It is because of the much lower decarburization level and

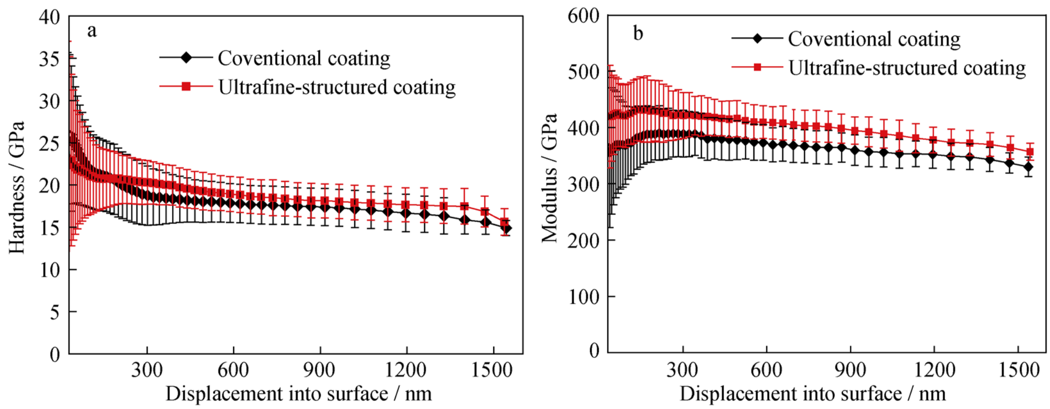

Fig. 5 Measured results by nanoindentation tests on top surfaces of coatings: **a** hardness and **b** modulus

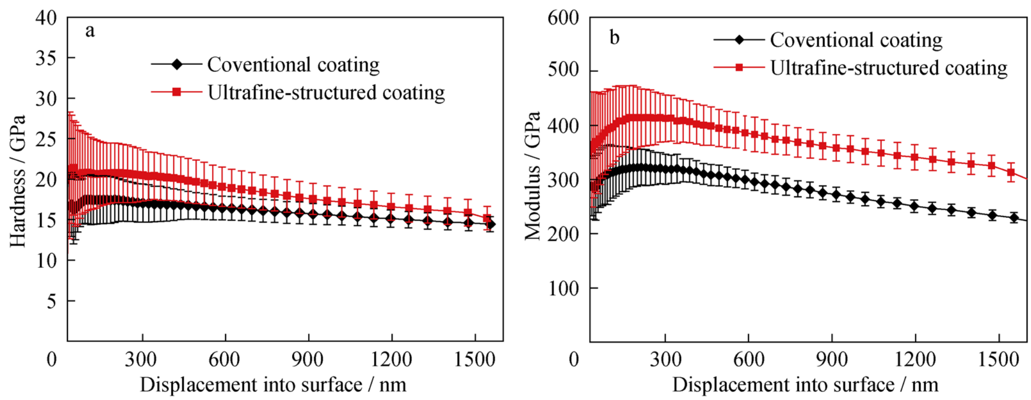

Fig. 6 Measured results by nanoindentation tests on cross sections of coatings: **a** hardness and **b** modulus

porosity of the ultrafine-structured coating that has 30 % higher cross-sectional elastic modulus than that of the conventional coating, which further contributes to the higher bond strength between splats and better wear resistance.

To better understand the wear mechanism of coatings, the worn surfaces were observed by SEM, as shown in Fig. 7. Obviously, there are many pits in the conventional coating after wear test, which are formed after the local spalling of materials under the action of abrasives. Also, there are other regions with little damage. This is mainly because of the inhomogeneous distribution of decarburized phases. In the regions with large W_2C phase, the removal of the coating materials is related to the crack in the binder phase (which becomes brittle due to the dissolution of W and C atoms or the amorphous state), the fracture of carbides under the action of the abrasive, and the disruption of the interfaces between the carbides and the binder phase [16–18]. There are few pits appearing in ultrafine-structured coating after wear, whereas the binder phase is almost removed by the cutting action of abrasives leading to the exposure of hard phases. This further confirms that the prepared ultrafine-structured coating has better uniformity and higher bond strength between splats, which results from the inhibited decarburization of coating.

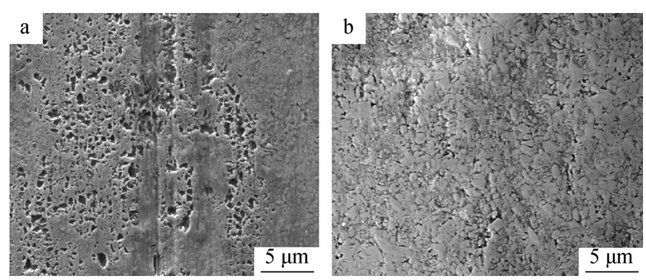

Fig. 7 SEM images of worn surfaces of two HVOF-sprayed coatings: **a** conventional WC–Co coating and **b** ultrafine-structured WC–Co coating

4 Conclusion

In this study, the effect of decarburization on the mechanical properties of HVOF-sprayed ultrafine-structured and conventional WC–Co coatings was investigated, in order to achieve better understanding of the microstructure and properties in cermet coating materials.

The prepared ultrafine-structured WC–Co coating has much higher density, which can be attributed to the better spreading characteristic of ultrafine composite powder particles. The decarburization of the ultrafine-structured WC–Co coating is effectively inhibited by reducing the tendency of exposure of WC particles to the ambient oxygen, which can be realized through the optimization of feedstock powder and spraying conditions. Both the hardness and modulus values measured on the top surface and cross section of coatings increase by inhibiting the WC decarburization. The wear resistance of thermal-sprayed cermet coatings greatly depends on the cross-sectional hardness and modulus, which reflects the bond strength between splats to some extent.

Acknowledgments This study was financially supported by the National High Technology Research and Development Program of China (No. 2013AA031104).

References

[1] Jing QF, Tan YF. Tribological properties of cobalt-based alloy coating with different cobalt contents by electro-spark deposition. Rare Met. 2013;32(1):40.

[2] Liu SL, Zheng XP, Geng GQ. Influence of nano-WC–12Co powder addition in WC–10Co–4Cr AC-HVAF sprayed coatings on wear and erosion behavior. Wear. 2010;269(5–6):362.

[3] Wang HB, Song XY, Liu XM, Wei CB, Gao Y, Fu J. Effect of heat-treatment of spray-dried powder on properties of ultrafine-structured WC–Co coating. Surf Coat Technol. 2012;207:117.

[4] Afzal M, Ajmal M, NusairKhan A, Hussain A, Akhter R. Surface modification of air plasma spraying WC–12% Co cermet coating by laser melting technique. Optics Laser Technol. 2014;56:202.

[5] Shipway PH, Gupta K. The potential of WC–Co hardmetals and HVOF sprayed coatings to combat water-droplet erosion. Wear. 2011;271(9–10):1418.

[6] Mateen A, Saha GC, Khan TI, Khalid FA. Tribological behaviour of HVOF sprayed near-nanostructured and microstructured WC–17 wt% Co coatings. Surf Coat Technol. 2011;206(6):1077.

[7] Wang HB, Song XY, Liu XM, Gao Y, Wei CB, Wang Y, Guo GS. Effect of carbon content of WC–Co composite powder on properties of cermet coating. Powder Technol. 2013;246:492.

[8] Fauchais P, Montavon G, Bertrand G. From powders to thermally sprayed coatings. Therm Spray Technol. 2010;19(1–2):56.

[9] Yin B, Zhou HD, Yi DL. Microsliding wear behavior of HVOF sprayed conventional and nanostructured WC–12Co coatings at elevated temperatures. Surf Eng. 2010;26(6):469.

[10] Basak AK, Celis JP, Vardavoulias M, Matteazzi P. Effect of nanostructuring and Al alloying on friction and wear behaviour of thermal sprayed WC–Co coating. Surf Coat Technol. 2012;206(16):3508.

[11] Babu PS, Basu B, Sundararajan G. Abrasive wear behavior of detonation sprayed WC–12Co coatings: influence of decarburization and abrasive characteristics. Wear. 2010;268(11–12):1387.

[12] Saha GC, Khan TI. Comparative abrasive wear study of HVOF coatings obtained by spraying WC–17Co microcrystalline and duplex near-nanocrystalline cermet powders. Eng Mater Technol. 2011;133(4):041002.

[13] Liu WB, Song XY, Zhang JX, Zhang GZ, Liu XM. Preparation of ultrafine WC–Co composite powder by in situ reduction and carbonization reactions. Refract Metals Hard Mater. 2009;27(1):115.

[14] Wang HB, Song XY, Wei CB, Gao Y, Guo GS. Abrasion resistance enhancement of ultrafine-structured WC–Co coating fabricated using in situ synthesized composite powder. Mater Sci Technol. 2013;29(11):1067.

[15] Rayon E, Bonache V, Salvador MD. Hardness and Young's modulus distributions in atmospheric plasma sprayed WC–Co coatings using nanoindentation. Surf Coat Technol. 2011;205(17–18):4192.

[16] Lu XH, Gao Y, Wei WZ, Zhang GY, Cai HW, Wang CG. Abrasive wear resistance of surface rare-earth high speed steel. Chin J Rare Met. 2013;37(1):744.

[17] He JH, Schoenung JM. A review on nanostructured WC–Co coatings. Surf Coat Technol. 2002;157(1):72.

[18] Lu L, Ma Z, Wang FC, Liu YB. Friction and wear behaviors of Al_2O_3–13 wt% TiO_2 coatings. Rare Met. 2013;32(1):87.